Chapter 4

Influence of Waveguide Structure on Spectral Characteristics of Evanescent Wave Fiber Components

4.1 Overview

The waveguide structure of evanescent wave fiber components is important to their dispersion characteristics. For fused-tapered fibers, the length, diameter, strain, bending, and dopant diffusion are the key issues for waveguide structures. For side-polished fibers, the polishing depth and radius of curvature are the controlling parameters of waveguide structures. The influence of waveguide structure on spectral characteristics can make a fiber device become more dispersive or, by contrast, less dispersive.

4.2 Side-Polished Endlessly Single-Mode Photonic Crystal Fibers

In this section, I will discuss the influence of the waveguide structure on spectral responses of the side-polished photonic crystal fiber and the fabrication method. Unlike the fused-tapering technique, side-polishing does not introduce significant fundamental mode cutoff loss. Therefore, variant kinds of novel

photonic crystal fiber devices can be fabricated based on side-polishing technique.

4.2.1 Higher Order Modes Excitation

Endlessly single-mode photonic crystal fibers [1-3] have been recently studied for ultra wide-band and high power guiding purposes as they can support only one transverse mode in an arbitrarily large mode field diameter (MFD). Moreover, the MFD is almost wavelength-independent [4] ascribing to that the air hole tubes confine the near-infrared long wavelengths much more effectively than the visible short wavelengths. The air holes control the waveguide dispersion primarily in the region of long wavelengths while the core material dominates the material dispersion over the entire range of wavelengths. Consequently, the waveguide and material dispersions can be effectively modified by varying the air hole size for near-infrared wavelengths [4,5] and by selecting the suitable core material for visible wavelengths [6], respectively. Since side-polishing does not substantially deform the air holes or the photonic bandgap structures [7], and as there is no strong deviation from the original dispersion characteristics of a photonic crystal fiber (PCF), it is a preferred fabrication method compared with the fused-tapering technique [8,9] for PCF components. In our previous work [7], the side-polishing technique was employed to achieve a wideband tunable PCF filter based on the material dispersion discrepancy between a side-polished endlessly single-mode photonic crystal fiber (SP-PCF) and a polymer overlay. In addition, side-polishing was also used to fabricate tunable PCF wideband couplers [10]. Nevertheless, the

holey cladding structure of a SP-PCF changes in a small local area with polishing-depth and radius of curvature R to vary the MFD, evanescent coupling, waveguide losses, dispersion slopes and to excite the higher-order modes. The waveguide dispersion of the SP-PCF is thus locally varied and these phenomena are fundamentally crucial to the spectral characteristics of all kinds of PCF components. In this work, the spectral responses in SP-PCFs to variations of the holey cladding structure due to side-polishing are investigated.

A SP-PCF is obtained by gradually removing a portion of holey cladding until the strong evanescent field is accessed. To put it simply, the removed holey cladding in a SP-PCF can be represented virtually as overlapped larger air holes with the same air hole pitch Λ in an unpolished PCF, as schematically shown in Figs. 4.1(a) and 4.1(b). Instead of the original air hole diameter d, the virtual air hole diameter ϕ gradually expands with increasing polishing-depth to change the effective refractive index dispersion (ERID) of a PCF. Since the holey cladding structure is locally changed, the resulting waveguide dispersion will be different from the original dispersion. Accordingly, the increase in the virtual relative hole diameter ϕ/Λ will not only make the ERID of near-infrared long wavelengths more dispersive [4,5], but also it will slowly extend the influence of waveguide dispersion toward visible short wavelengths, which excites higher-order modes as a result [4].

In fabrication, the endlessly single-mode photonic crystal fiber (ESM-12-01: CRYSTAL FIBRE A/S) with triangular array air hole tubes has the core, cladding and air hole diameters of 12 μm, 125 μm and 3.68 μm, respectively. The Λ is 8 μm and the d/Λ is 0.46. A section of jacket of the PCF was striped off and the bare section was then embedded and glued into a curved Si V-groove with different R [7]. The Si V-grooves were precisely etched for

remained central holey cladding at specified depths *h* [11]. The exposed holey cladding was removed by using a polishing slurry with a particle size of around 60 nm in order to avoid optical losses resulting from roughness scattering. However, the air hole tubes were broken during polishing and were infiltrated by slurry and this resulted in huge optical losses. The incoming fluid was purged using compressed air flow and the SP-PCF was then baked in an oven at 150°C for around 30 minutes. The cross-sectional views shown in Fig. 4.1(c) are from one of the polished ESM-12-01 fibers and are presented here to verify that the incursive materials were cleaned away.

In Fig. 4.2, the fundamental-mode cutoff induced by the fused-tapering technique in references [8,9] does not occur in the loss spectra of SP-PCFs with R = 800 cm. This shows that side-polishing does not substantially change the dispersion characteristics of the PCF components. The waveguide loss increases and becomes more dispersive with increases in polishing-depth and wavelength. For the inset picture shown in Fig. 4.2, although a substantial portion of core was polished away, where the polished surface is beneath the core's top boundary and thus h is -8.2 μm, Fig. 4.2 shows that a moderate fraction power of the wavelength ~ 1.25 μm can still be guided. On the other hand, a 532 nm laser light (Nd:YVO4) was launched into the SP-PCFs to observe the variations of the far-field mode patterns shown in Fig. 4.3 for visible short wavelengths. When the polishing-depth was increased, the confined optical power was gradually coupled to the air filling modes resulting in the MFD being expanded. This coupling process eventually excites the higher-order modes and induces huge optical losses. In Figs. 4.3(b) and 4.3(c), the MFDs are different at 532 nm and 633 nm (He-Ne) wavelengths even though the same holey cladding thickness is maintained. By contrast, the MFD

in an endlessly single-mode PCF is no longer wavelength-independent due to the changed holey cladding structure. The higher-order mode patterns are not similar to that of the hexagonal symmetric PCFs [1] since the polished fiber is not cylindrically symmetric and thus the mode patterns behave as speckles. When the polishing-depth was increased, the interfered speckles became even chaotic since more higher-order modes were excited and thus the influence of the changed waveguide dispersion was extended to the visible short wavelengths. The varied holey cladding structure excites many more higher-order modes at 532 nm than at 633 nm wavelength. Although the mode pattern in Fig. 4.3(b) shows more speckles than that in Fig. 4.3(c), the speckles could not be clearly discerned and recorded by our 4-Mega-pixel digital camera. From Figs. 4.2 and 4.3 it can be seen that when a small portion of the core was polished, the near-infrared long wavelengths at the communication bands began to suffer losses. However, when a substantial portion of the core was further polished away, as shown in the inset in Fig. 4.2, the visible short wavelengths could still be effectively guided though multi-mode in nature, as shown in Fig. 4.3(d). This is quite different from the standard single-mode fiber where all guiding wavelengths suffer catastrophic optical losses when the core is polished to the point where it is exposed to air. For a deep-polished PCF as Fig. 4.1(b), the effective guiding area of the longer wavelengths at near-infrared will expand downward to beyond the core boundary and will cover part of the nearby holey cladding. Therefore, it is shown that the original waveguide dispersion primarily contributes to the near-infrared long wavelengths rather than to the visible short wavelengths in an un-polished state. In brief, the deeper polishing-depth makes the ERID more dispersive at

near-infrared long wavelengths and makes the higher-order modes excited at visible short wavelengths.

4.2.2 Dispersion Slope

Since a dispersion measurement instrument was not available to directly measure the dispersion of a SP-PCF in this work, in order to investigate the influence of R in a SP-PCF, observations on variations of the slope of the fundamental-mode cutoff curve [7] were employed. The dispersive optical polymer OCK-433 (Nye Lubricants) was applied on SP-PCFs to obtain a fundamental-mode cutoff, shown as transmission losses in Figs. 4.4(a) and 4.4(b), resulting from the material dispersion discrepancy between the SP-PCF and polymer overlay. The fundamental-mode cutoff wavelength could be thermally tuned [7,11]. The typical R of the side-polished fibers with glass substrates was 25 cm ~ 50 cm [10] and the R in our SP-PCFs using precision silicon V-groove substrates were 1,500 cm and 800 cm, respectively. A larger R will generate a longer effective interaction length L_{eff} in which a longer wavelength experiences a longer L_{eff} than a shorter wavelength since L_{eff} is proportional to the square root of the wavelength [12]. In this work, the evanescent field of SP-PCF was found to be accessible when h reached the first ring of the air holes at around 1.8 um. The evanescent field of the SP-PCFs is much more strongly localized than that of standard polished single-mode fibers. From Figs. 4.4(a) and 4.4(b), it can be seen that the SP-PCF in the air with a smaller R shows a greater dispersive insertion losses, whereas the SP-PCF with an optical polymer overlay and a larger R presents a much steeper

fundamental-mode cutoff. These are important issues for evanescent coupling of PCF components and the explanations are as follows. The smaller R means a greater degree of fiber bending for longer wavelengths and a deformation of the electromagnetic field distribution as it moves towards the outside of the bend [13]. Moreover, the holey cladding structure will vary much more quickly along the polishing length for longer wavelengths in terms of ϕ/Λ. Consequently, this structure will induce more serious optical losses for longer wavelengths and the insertion loss spectra become more dispersive. On the other hand, a SP-PCF with a larger R produces a longer L_{eff} for guiding wavelengths to interact with a longer length of dispersive optical polymer. Therefore, the longer wavelengths will suffer more optical losses than the shorter wavelengths to give rise to a steeper fundamental-mode cutoff while propagating through the whole L_{eff}. In short, it is clear that the coupling characteristics of fiber couplers using SP-PCFs are definitely related to the R of SP-PCFs. Moreover, the zero dispersion wavelength of a PCF can be moved when the air hole size varies [14]: this implies that different polishing-depths may induce shifts in the zero dispersion wavelength of the SP-PCFs. This work can be carried out once a dispersion measurement instrument is made available.

In summary, we have demonstrated that the structure of a holey cladding is important to the spectral characteristics of SP-PCFs. The spectral characteristics of SP-PCFs are very different from those of side-polished standard single-mode fibers. Furthermore, side-polishing does not introduce significant fundamental-mode cutoff loss in PCF components whereas the polishing-depth and curvature radius can change the waveguide dispersion. Also, the evanescent field is very strongly localized and a deeper polishing-depth or a larger curvature radius can give rise to a more dispersive

spectral characteristic. Finally, the higher-order modes can be excited at the visible short wavelength end. These are important issues for the design of novel ultra-wideband photonic crystal fiber components.

References

[1] P. Russell, “Photonic crystal fibers,” Science **299**, 358-362 (2003).

[2] T. A. Birks, J. C. Knight, and P. St. J. Russell, “Endlessly single-mode photonic crystal fiber,” Opt. Lett. **22**, 961-963 (1997).

[3] K. Saitoh, Y. Tsuchida, M. Koshiba, and N. A. Mortensen, “Endlessly single-mode holey fibers: the influence of core design” Opt. Express. **13**, 10833-10839 (2005).

[4] M. Koshiba and K. Saitoh, “Applicability of classical optical fiber theories to holey fibers,” Opt. Lett. **29**, 1739-1741 (2004).

[5] N. A. Mortensen, M. D. Nielsen, J. R. Folkenberg, A. Petersson, and H. R. Simonsen, “Improved large-area endlessly single-mode photonic crystal fibers,” Opt. Lett. **28**, 393-395 (2003).

[6] B. J. Mangan, J. Arriaga, T. A. Birks, J. C. Knight, and P. St. J. Russell, “Fundamental-mode cutoff in a photonic crystal fiber with a depressed-index core,” Opt. Lett. **26**, 1469-1471 (2001).

[7] N. K. Chen and S. Chi, “Evanescent wave photonic crystal fiber tunable filter using dispersive optical polymers,” in *Optical Fiber Communication Conference OFC’05 (Optical Society of America, Washington, D.C., 2005)*, paper OWD3.

[8] H. C. Nguyen, B. T. Kuhlmey, M. J. Steel, C. L. Smith, E. C. Mägi, R. C.

McPhedran, and B. J. Eggleton, “Leakage of the fundamental mode in photonic crystal fiber tapers,” Opt. Lett. **30**, 1123-1125 (2005).

[9] E. C. Mägi, P. Steinvurzel, and B. J. Eggleton, “Tapered photonic crystal fibers,”Opt. Express **12**, 776-784 (2004).

[10] H. Kim, J. Kim, U. C. Paek, B. H. Lee, and K. T. Kim, “Tunable photonic crystal fiber coupler based on a side-polishing technique,” Opt. Lett. **29**, 1194-1196 (2004).

[11] N. K. Chen, S. Chi, and S. M. Tseng, “An efficient local fundamental-mode cutoff for thermo-optic tunable Er^{3+}-doped fiber ring laser,” Opt. Express. **13,** 7250-7255 (2005).

[12] M. J. F. Digonnet and H. J. Shaw, “Analysis of a tunable single mode optical fiber coupler,” IEEE J. Quantum Electron. **QE-18**, 746-754 (1982).

[13] F. Wassmann, “Modal field analysis of circularly bent single-mode fibers,” J. Lightwave Technol. **17,** 957-968 (1999).

[14] K. L. Reichenbach and C. Xu, “The effects of randomly occurring nonuniformities on propagation in photonic crystal fibers” Opt. Express. **13,** 2799-2807 (2005).

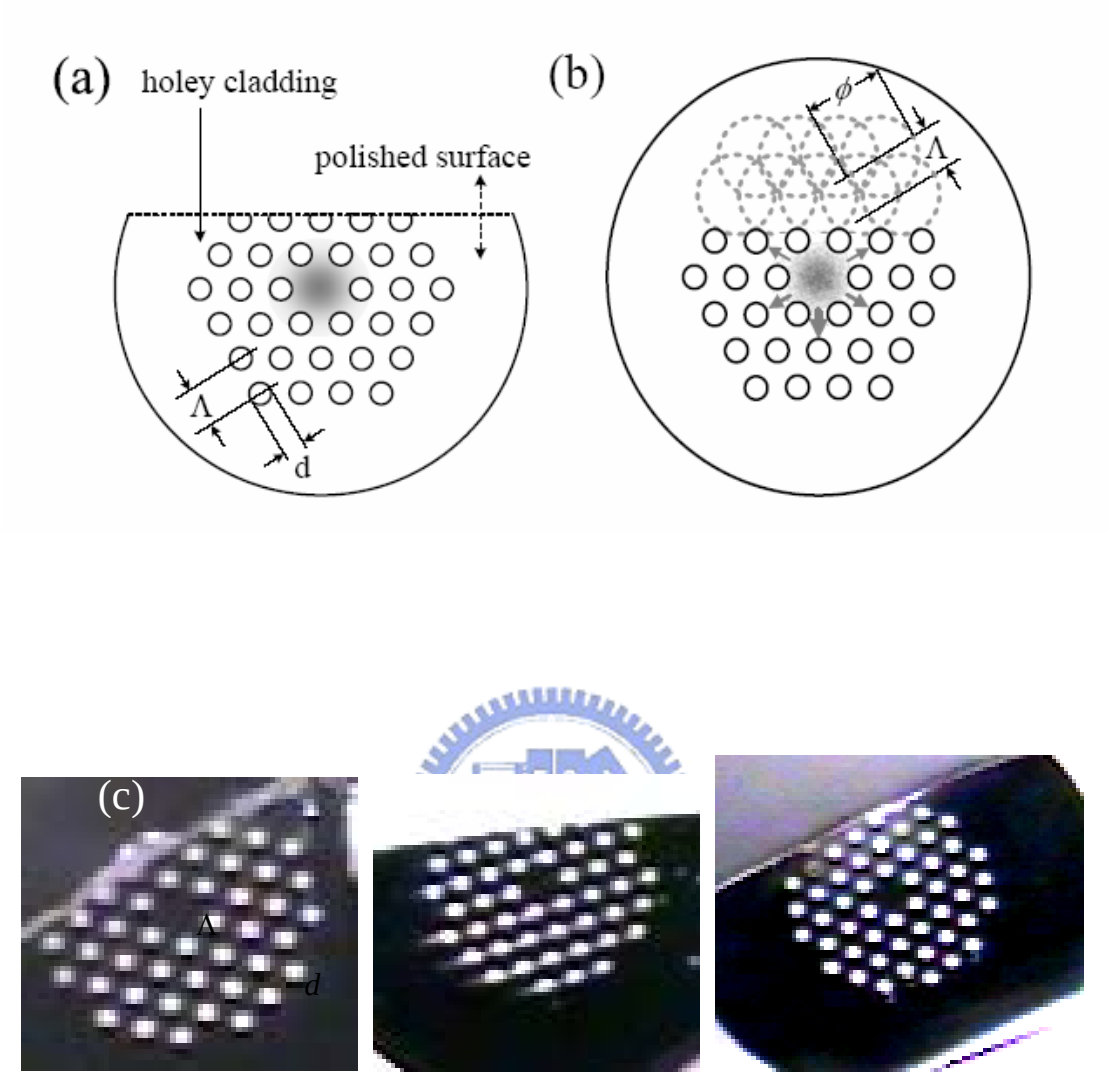

Fig. 4.1 (a) SP-PCF can be represented virtually as an unpolished PCF with variable larger air holes (dashed circles) in (b). (c) Cross-sectional views of the polished ESM-12-01 fiber under 1000× CCD microscope from the polishing center (left) toward the polishing boundary (right).

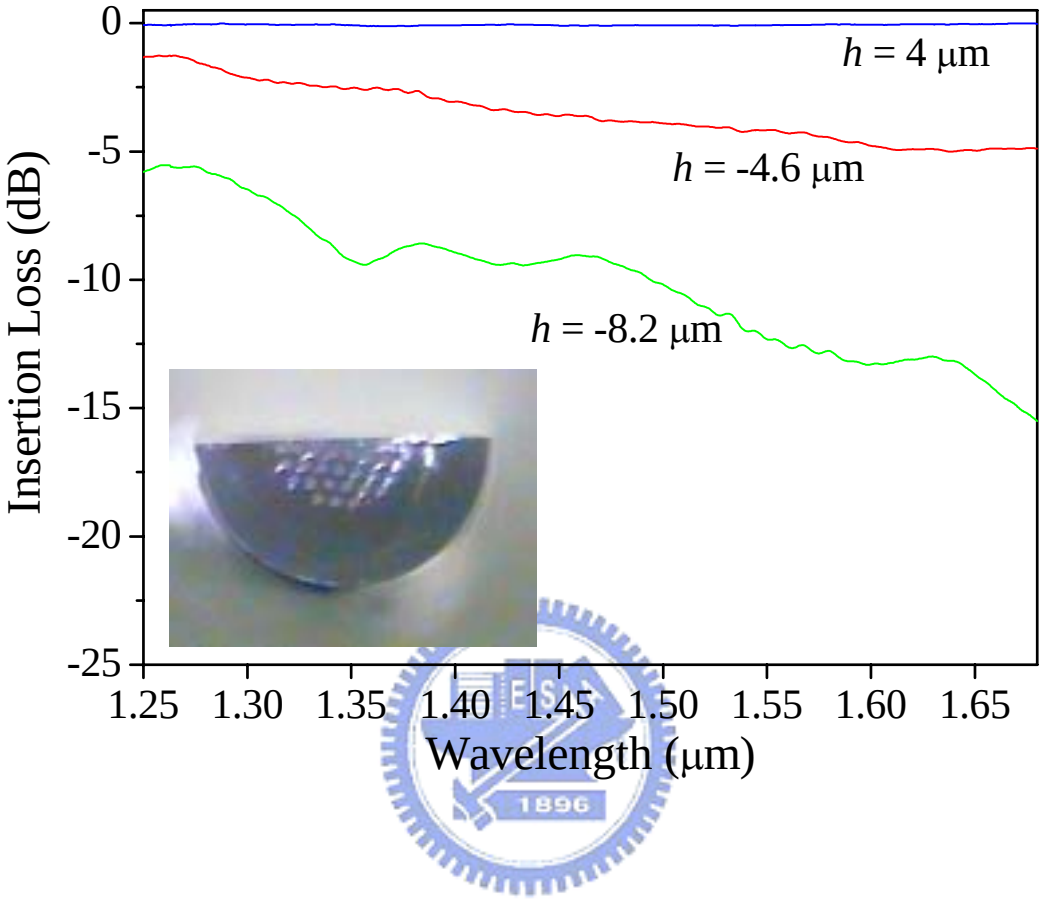

Fig. 4.2 Loss spectra of the SP-PCF with R = 800 cm at different remained holey cladding depths. The inset picture shows the central cross-sectional view of the SP-PCF at h = -8.2 μm and where a substantial portion of the core was polished away.

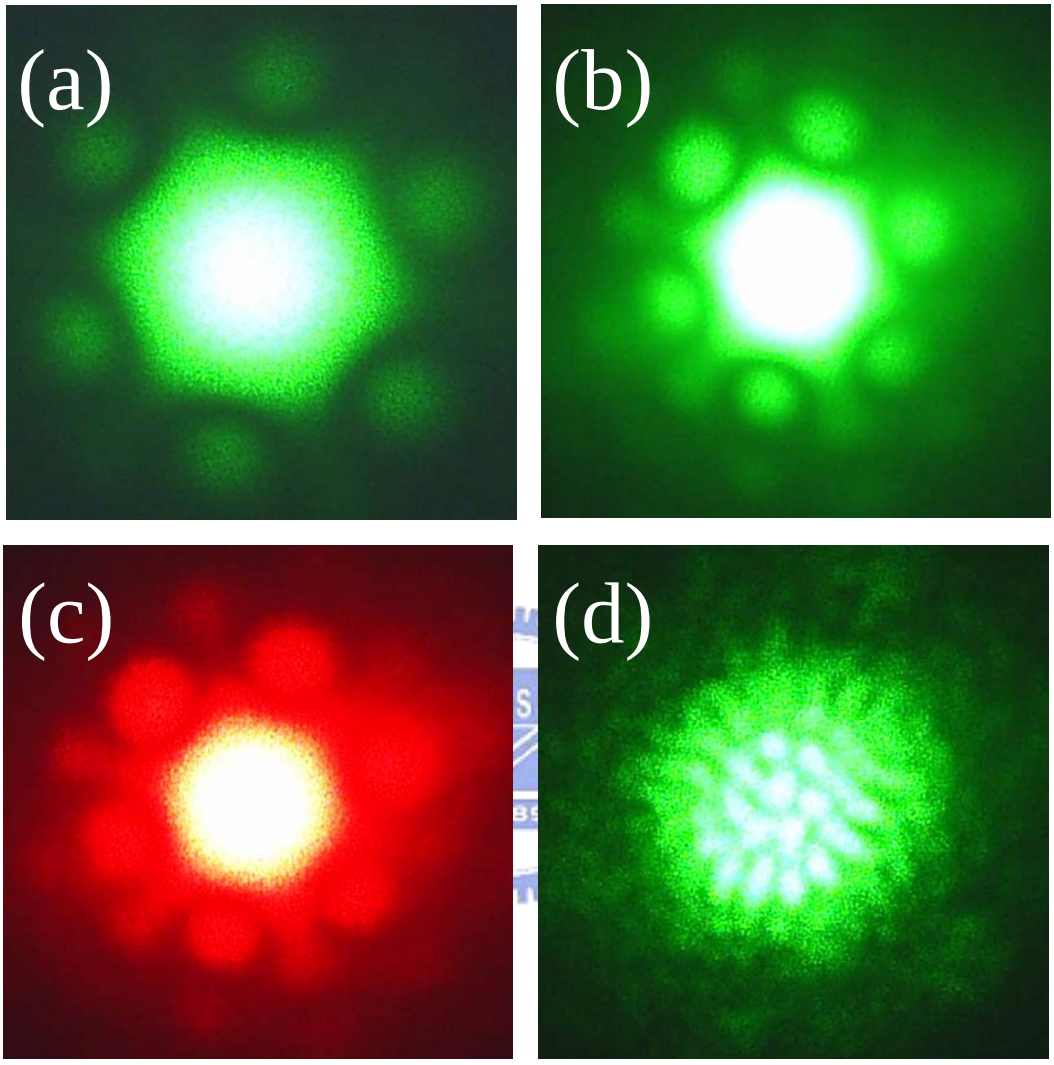

Fig. 4.3 Far-field mode patterns from the output end of SP-PCFs (R = 800 cm) that are 10 cm away from the polishing center at the wavelength and with various h measurements: (a) 532 nm & 4 μm, (b) 532 nm & -4.6 μm, (c) 633 nm & -4.6 μm, and (d) 532 nm & -8.2 μm.

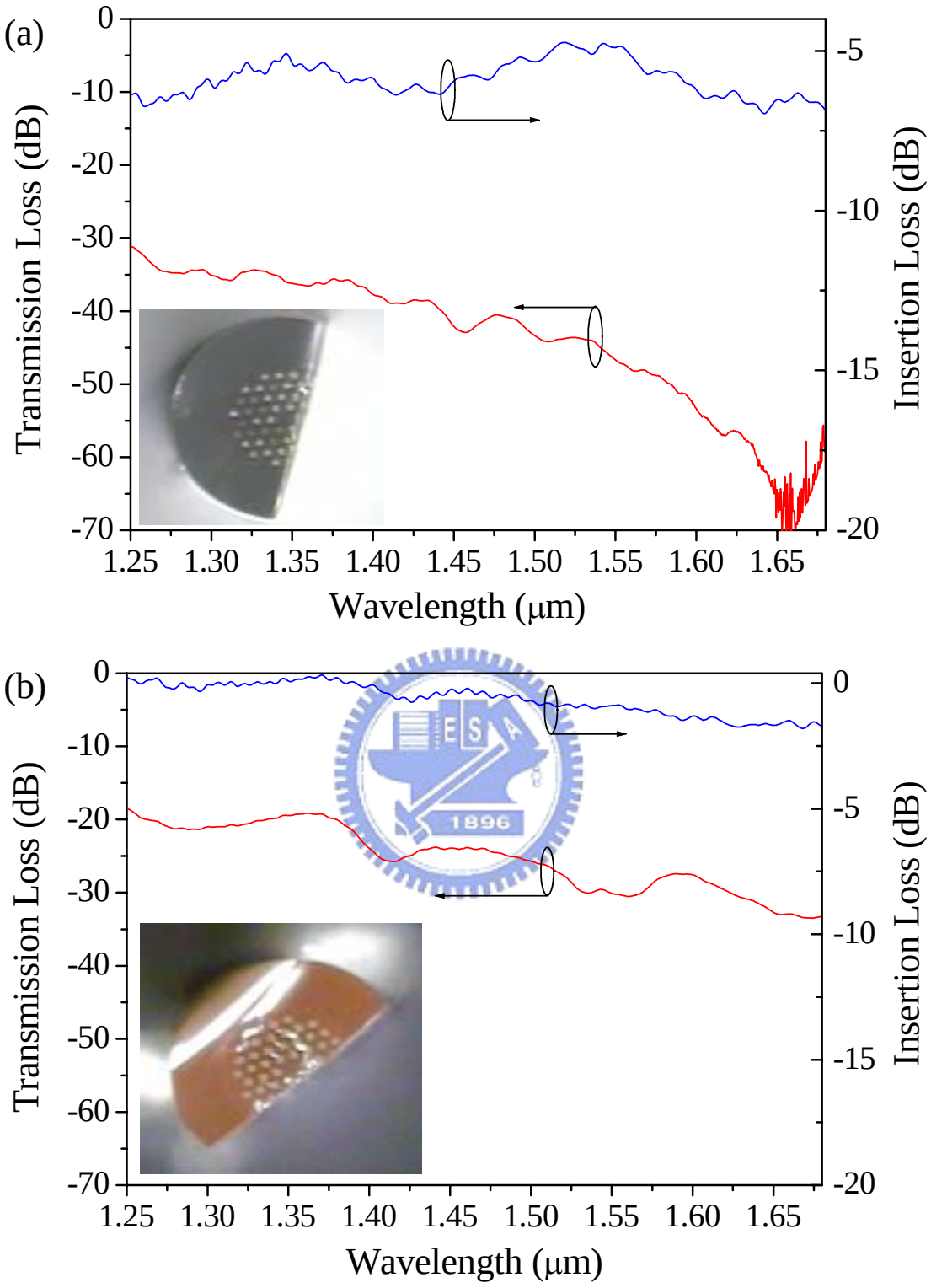

Fig. 4.4 Spectral responses of SP-PCFs with h ~ 1.8 μm and R of (a) 1500 cm and (b) 800 cm using OCK-433 dispersive polymer overlay at a temperature of 60°C. The blue and red lines are transmission losses of SP-PCFs in air and with a polymer overlay, respectively.